Effect of Extrusion Pressure and Lipid Properties on the Size and Polydispersity of Lipid Vesicles

D. G. Hunter and B. J. Frisken
Department of Physics, Simon Fraser University, Burnaby, British Columbia V5A 1S6, Canada

ABSTRACT The production of vesicles, spherical shells formed from lipid bilayers, is an important aspect of their recent application to drug delivery technologies. One popular production method involves pushing a lipid suspension through cylindrical pores in polycarbonate membranes. However, the actual mechanism by which the polydisperse, multilamellar lipid suspension breaks up into a relatively monodisperse population of vesicles is not well understood. To learn about factors influencing this process, we have characterized vesicles produced under different extrusion parameters and from different lipids. We find that extruded vesicles are only produced above a certain threshold extrusion pressure and have sizes that depend on the extrusion pressure. The minimum pressure appears to be associated with the lysis tension of the lipid bilayer rather than any bending modulus of the system. The flow rate of equal concentration lipid solutions through the pores, after being corrected for the viscosity of water, is independent of lipid properties.

INTRODUCTION

Vesicles are quasispherical structures composed of lipid bilayers that encapsulate an aqueous space. They can be prepared in the laboratory by various methods including reverse phase evaporation, detergent dialysis, and extrusion (New, 1995). They have applications in research laboratories as model membranes and in the pharmaceutical industry as drug delivery agents. In this paper we will focus on the method of preparing samples of large unilamellar vesicles by extrusion through small pores (Hope et al., 1985). In this process, solutions containing extremely large ($\geq 1\ \mu$m) multilamellar vesicles are forced or extruded through pores with diameters on the order of 100 nm, using either a pressurized gas (Hope et al., 1985) or a syringe-based plunger system (MacDonald et al., 1993). This method is widely used in research and pharmaceutical applications because it is a relatively fast way to produce a roughly monodisperse vesicle population of controlled average size without the introduction of contaminants. Monodisperse samples are desirable because the circulation lifetime of drug-encapsulated vesicles is size dependent (Woodle et al., 1995).

Early characterization of extruded vesicles by electron microscopy (EM) (Hope et al., 1985) showed that extrusion of lipid solution through 100-nm pores resulted in an average vesicle size of 140 nm with standard deviations of ~40 nm. Multiple passes through the extrusion device were shown to reduce the multilamellarity of the vesicles. Further studies investigated vesicles resulting from extrusion through different pore sizes (Mayer et al., 1986) and from extrusion of different lipids at various temperatures (Nayer et al., 1989). Characterization by EM and dynamic light scattering (DLS) showed that, while extrusion through 100-nm pores resulted in ~100-nm vesicles, extrusion through larger pores generally yielded vesicles smaller than the pore size, and extrusion through smaller pores yielded vesicles larger than the pore size (Mayer et al., 1986). Results for different lipids indicated that the final vesicle size might be lipid-dependent (Nayer et al., 1989). Extrusion was found to be unsuccessful below the gel-fluid transition temperature, an effect that was attributed to decreased fluidity of the membrane below the transition temperature (Nayer et al., 1989). Later studies investigated the effect of extrusion pressure and lipid concentration on vesicle size over limited ranges of pressure and concentration (Küolchens et al., 1993). Whereas no effect on size due to concentration was observed in these studies, there was some evidence that the size of the vesicles decreased slightly with increasing extrusion pressure.

The actual mechanism by which the large, polydisperse, multilamellar vesicles break up into smaller, unilamellar, and basically monodisperse vesicles remains unclear. Description of this process should lead to an understanding of how extrusion parameters and lipid properties affect the size and polydispersity of the extruded samples. One proposed mechanism for vesicle formation (Clerc and Thompson, 1994) is based on the breakup of cylindrical phospholipid bilayer structures of radius R outside the pores into smaller cylindrical structures of length λ, where $\lambda = 2\pi R$. However, this predicts a vesicle size that is larger than is generally observed and does not account for variations of vesicle size with extrusion pressure or lipid properties. Several recent theoretical studies have examined vesicles in pores or under shear. However, although they involve issues related to those found in vesicle extrusion, they do not address the extrusion process directly. Gompper and Kroll (1995) model the mobility of vesicles in pores as a function of a driving field. The model considers vesicles larger than the pore diameter, which must deform to enter the pore. The deformation of the vesicles is assumed to be governed by bending energies only, and the mobility is found to depend on the bending energies of the

Received for publication 18 July 1997 and in final form 6 March 1998.

Address reprint requests to Dr. Barbara Frisken, Department of Physics, Simon Fraser University, Burnaby, BC V5A 156, Canada. Tel.: 604-291-5767; Fax: 604-291-3592; E-mail: frisken@sfu.ca.

0006-3495/98/06/2996/07 $2.00

bilayer. Bruinsma (1996) focuses on the flow of vesicles inside cylindrical pores and shape deformations that might occur inside the pore. He finds that the rheological properties of the vesicles are independent of the bending energy. Both of these studies focus on the effect of bending energies only and do not allow for rupture of the vesicles.

In this paper we report studies of the size and polydispersity of extruded vesicles as a function of extrusion pressure and lipid properties. Lipid solutions with a concentration of 1 mg/ml were extruded through polycarbonate membranes with a nominal pore diameter of 100 nm. We observe that as the applied pressure is increased, the size of the extruded vesicles decreases, but the size of vesicles extruded at a given pressure does not depend significantly on the temperature at which the vesicles are extruded or the lipid used. The relative polydispersity does not change with applied pressure, temperature, or lipid. At high pressures, the pressure dependence of the flow rate corrected by the viscosity is independent of phospholipid properties. However, there exists a minimum pressure for extrusion below which it is not possible to force the vesicles through the pores of the filter membrane. This minimum pressure depends on the type of lipid being extruded and is found to be consistent with the lysis tension required to rupture the phospholipid membrane, rather than any bending energy of the system.

THEORETICAL CONSIDERATIONS

Assuming laminar flow, the rate of flow of volume q of a viscous fluid through a cylindrical channel is given by (Landau and Lifshitz, 1987)

$$q = \frac{\pi R^4}{8\eta}\left(\frac{\Delta P}{\Delta L}\right), \tag{1}$$

where R is the radius of the channel, η is the viscosity of the fluid, ΔL is the length of the channel, and ΔP is the pressure difference between the ends of the channel. To relate q to the observed flow rate Q of fluid through the pores of a polycarbonate filter, we assume that all of the pores are the same size and multiply q by the number of pores per unit area N and the usable area A of the membrane, so that $Q = NAq$. Equation 1 can also be expressed as Darcy's law,

$$\eta Q = K\left(\frac{\Delta P}{\Delta L}\right), \tag{2}$$

where K is the permeability of the filter. The viscosity-corrected flow rate ηQ should be independent of temperature and linear in the pressure difference. Measurement of the flow rate as a function of pressure or channel length will then give the value of the filter permeability K.

The preceding formulae assume that the fluid is homogeneous, with no impurities or suspended bodies that might affect the flow. This is obviously not true for the case of suspended vesicles being forced through small pores. Corrections must be made to account for the presence of these bodies in the fluid.

Bruinsma (1996) has recently published a study of the flow of vesicles in pores. He finds that at large applied pressures, Darcy's law is obeyed with an effective permeability K_{eff}, which depends on the number of vesicles per unit length in the pore n, the length of the vesicle L^*, and the radius of the pore R_p:

$$K_{\text{eff}} = \frac{NA\pi R_p^4}{8 + 0.233 \times (nL^*)(L^{*2}/R_p^2)}. \tag{3}$$

A schematic diagram of a vesicle in a pore is shown in Fig. 1. The only characteristic of the lipid mixture that K_{eff} depends on is the number of vesicles in the pore, and so the permeability should still be independent of temperature. Derivation of Eq. 3 involves consideration of the thickness of a lubrication layer h^* between the vesicle and the wall of the pore and the assumption that $h^* < L^*$. The thickness of the lubrication layer is a function of the velocity V of the vesicle in the pore and is given by

$$h^*(V) = 2.05 \times R_p\left(\frac{\eta V}{\gamma}\right)^{2/3}, \tag{4}$$

where γ is the surface tension in the lipid bilayer. As h^* increases, the radius of the vesicle in the pore will decrease. Physically, the radius cannot decrease indefinitely, so some limit on the thickness of the lubrication layer should be imposed. At smaller applied pressures, the model predicts that the vesicle moves slowly and violates Darcy's law. The flow rate is predicted to reach zero at zero applied pressure head, i.e., no minimum pressure is expected.

A second model studying vesicles in pores (Gompper and Kroll, 1995) uses Monte Carlo simulations to study the dependence of the mobility of model vesicles on the pore radius, the

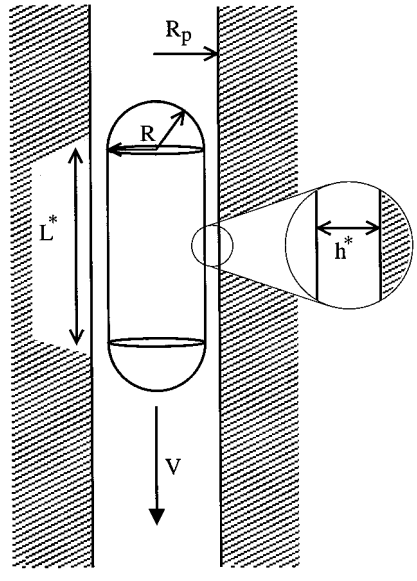

FIGURE 1 Schematic diagram of a vesicle in a pore of radius R_p. The vesicle is a spherocylinder of length L^* and end-cap radius R. The vesicle moves through the pore at a velocity V and is separated from the pore wall by a lubrication layer of thickness h^*.

vesicle size, and the bending energy of the lipid bilayer. The vesicles are modeled by a tethered network of sites on a closed surface. The simulations show that there is a minimum driving field required to insert the vesicles into the pores, and that this minimum field scales with the bending rigidity of the phospholipid membrane. The simulations also show that the mobility of the vesicle solution scales with the bending energy of the lipid bilayer. It should be noted that this model assumes that the vesicles are subject to a linear field gradient, which is physically different from an applied pressure difference (Gompper and Kroll, 1995).

MATERIALS AND METHODS

Preparation of phospholipid vesicles

The phospholipids used were 1,2-dimyristol-*sn*-phosphatidylcholine (DMPC), 1-stearoyl-2-oleoyl-*sn*-phosphatidylcholine (SOPC), and 1,2-dioleoyl-*sn*-phosphatidylcholine (DOPC) (Avanti Polar Lipids, Alabaster, AL) in powder form. For each sample, a single variety of phospholipid was hydrated, using purified water from a Milli-Q Plus water purification system (Millipore, Bedford, MA), in ratios of 1–2.5 mg of phospholipid per milliliter of water. Water from the Milli-Q Plus filtration was used to keep the concentration of contaminants in the vesicle solution negligible. This ensures that the vesicles will swell to spherical shapes after extrusion (Mui et al., 1993). The mixtures of water and phospholipid were taken five times through a freeze-thaw procedure. This procedure involved freezing the solution by immersion in liquid nitrogen, followed by thawing by immersion in 50°C water, followed by thorough vortexing.

After the freeze-thaw-vortex process, the vesicle suspension was cleaned and regularized by extruding it once through two polycarbonate membrane filters (Osmonics, Livermore, CA) with pore diameter 400 nm at 120 psi. This process, which we call preextrusion, was found to improve the repeatability of the results of the light scattering experiments and the measurements of the extrusion flow rate. After this step, light scattering measurements revealed very polydisperse samples with average radii of ~ 1 μm.

Before extrusion through the final filter size, the preextruded vesicle suspension was diluted with purified water to a concentration of 1 mg/ml of phospholipid in water. At this concentration, we expect that there will be an average of one vesicle present in any given pore during the extrusion process. The preextruded vesicle suspension was then extruded a minimum of 10 times through two polycarbonate membranes (Osmonics) with a nominal pore diameter of 100 nm, using an Extruder (Lipex Biomembranes, Vancouver, BC) by applying a pressure gradient. Water from an external water bath was circulated through the extruder to control the extrusion temperature. The pressure gradient across the membranes was created using prepurified, compressed N_2 gas. For each phospholipid, a series of extrusions was made at a range of pressures. The DMPC suspensions were extruded at pressures ranging from 30 psi to 300 psi at 25°C, 30°C, and 40°C. The SOPC and DOPC suspensions were extruded at 30°C, with pressures ranging from 300 psi down to 65 psi for DOPC and 50 psi for SOPC. The vesicle suspension was reextruded a minimum of 10 times, or until the macroscopic bulk flow rate became constant. The macroscopic bulk flow rate of the extruded suspension was measured either with a stopwatch and a graduated cylinder, or by observing a video recording of the flow into a graduated cylinder.

The polycarbonate membranes (Osmonics batch no. AE84AH11C007) used in these experiments had a nominal diameter of 100 nm. EM measurements made by the manufacturer of characteristic membranes from this batch show that there are pores distributed between 85 and 108 nm, with an average value of 93 nm. The pores are not perfectly cylindrical but are slightly barrel-shaped, being on the order of 10% greater in diameter in the center of the membrane than at the edges. This is due to the etching process used in the manufacture of the membrane, and is intentional on the part of the manufacturer, as it increases the rate of flow through the filters without increasing the size of the entry to the pore. The area of the membrane available for extrusion was 4.15 cm^2, and the pore density was 3.8×10^8 cm^{-2}.

Vesicle characterization by DLS and SLS

Vesicle size and polydispersity were characterized primarily by dynamic light scattering (DLS) measurements. These results were confirmed by static light scattering (SLS) measurements. The apparatus used for the light scattering experiments was an ALV DLS/SLS-5000 spectrometer/goniometer (ALV-Laser GmbH, Langen, Germany). Before size and size distribution analysis of the sample by DLS and SLS, the vesicle suspension was diluted in Milli-Q water to ~ 0.1 mg/ml and placed in a 10-ml cylindrical glass vial. The sample was placed in a toluene bath. The toluene bath was maintained at the temperature at which the vesicles were extruded, to minimize thermal expansion and/or contraction of the vesicles. The light source for the experiments was a helium-neon laser of wavelength 633 nm (SpectraPhysics 127-35, Mountain View, CA). Light from the laser passed through the sample, and light scattered by the sample was detected at angles of 60°, 90°, and 120° from the transmitted beam for DLS measurements and at 23 angles from 16° to 150° for SLS measurements by a photomultiplier tube (model 9130; EMI, Hayes, England).

DLS measurements involved analysis of the time autocorrelation of the scattered light, as performed by the digital correlator of the ALV DLS/SLS-5000 system. The normalized time autocorrelation function of the intensity of the scattered light $g^{(2)}(\tau)$ for a given time τ is given by (Berne and Pecora, 1976)

$$g^{(2)}(\tau) = \frac{\langle I(t)I(t+\tau)\rangle}{\langle I(t)I(t)\rangle}, \tag{5}$$

where $I(t)$ and $I(t+\tau)$ are the intensities of the scattered light at times t and $t+\tau$, respectively, and the braces indicate averaging over t. The intensity-intensity time autocorrelation function may also be expressed as

$$g^{(2)}(\tau) = 1 + \beta[g^{(1)}(\tau)]^2, \tag{6}$$

where

$$g^{(1)}(\tau) = \frac{\langle E(t)E^*(t+\tau)\rangle}{\langle E(t)E^*(t)\rangle} \tag{7}$$

is the time autocorrelation function of the electric field of the scattered light, and β is a factor that depends on the experimental geometry. Here $E(t)$ and $E(t+\tau)$ are the scattered electric fields at times t and $t+\tau$, respectively, and * denotes complex conjugates.

The time autocorrelation data provide information about diffusion in the sample, because $g^{(1)}(\tau) = e^{-Dk^2\tau}$ for monodisperse particles, where k is the magnitude of the scattering wave vector, and D is the diffusion coefficient. The Stokes-Einstein relation $D = K_B T/6\pi\eta R_h$ can be used to relate the diffusion coefficient to the hydrodynamic radius R_h of the particles, where K_B is Boltzmann's constant, T is the temperature in degrees Kelvin, and η is the dynamic viscosity.

For a polydisperse sample, $g^{(1)}(\tau)$ is no longer a single exponential. The effect of a distribution of decay rates on $g^{(1)}(\tau)$ is given by

$$g^{(1)}(\tau) = \int_0^\infty G(\Gamma)e^{-\Gamma\tau}d\Gamma, \tag{8}$$

where $\Gamma = Dk^2$ and $G(\Gamma)$ is the function describing the distribution of decay rates. The DLS data were analyzed primarily by using the method of cumulants (Koppel, 1972). (By using other methods (e.g., CONTIN), we determined that the distribution was not multimodal.) In this method, the electric field time autocorrelation function is expanded in terms of cumulants of the distribution:

$$g^{(1)}(\tau) = e^{-\bar{\Gamma}\tau+\mu\tau^2/2-\cdots}, \tag{9}$$

where $\bar{\Gamma}$ is the mean of Γ and μ is the variance of the distribution. Use of only these two parameters assumes that $G(\Gamma)$ is a Gaussian distribution.

A nonlinear least-squares fitting routine was used to fit the functional form obtained by combining Eqs. 6 and 9 to the DLS data to obtain $\bar{\Gamma}$ and μ. The hydrodynamic radius R_h was calculated from $\bar{\Gamma}$ using the Stokes-Einstein relation. Data taken at angles spanning the instrument's range were consistent with results expected for polydisperse samples. The measurements reported here were taken at 90°, where the effects of reflection and polydispersity are minimized. The hydrodynamic radius was measured five times at 90° for all samples. These five radii were averaged to find a mean radius $\bar{R}_h$. The standard deviation of the five radii was taken as an estimate of the uncertainty in $\bar{R}_h$. The variances of the five measurements were also averaged to find a mean variance $\bar{\mu}$. The standard deviation of the distribution σ was calculated from $\bar{\mu} = \sigma^2$.

The radii of the vesicles were also measured by analysis of the static light scattering data. A model function using the form factor for hollow spheres with finite thickness was fit to the data by a nonlinear least-squares fitting routine. The vesicle sizes obtained from fitting the SLS data agreed with the hydrodynamic radii determined from the DLS data.

RESULTS

Fig. 2 shows the radius, relative standard deviation of the vesicle size distribution, and the flow rate for a typical extrusion experiment. In this case, DMPC solution was extruded through 100-nm polycarbonate membrane filters at 200 psi and 30°C. As seen in Fig. 2 *a*, the radius decreases rapidly to ~120% of the pore radius in four extrusions. The radius relative to the pore radius is shown on the right-hand axis. After four extrusions, the size decreases more slowly, so that by the 10th extrusion, the vesicle radius is 12% larger than the pore radius. Similarly, the relative standard deviation $\sigma/\bar{\Gamma}$ (Fig. 2 *b*) decreases quickly with the first three extrusions and then levels off to a roughly constant level. As apparent from Fig. 2 *c*, there is no discernible trend in the flow rate over the series of extrusions. This behavior is typical of extrusions made at pressures greater than or equal to 100 psi. At lower applied pressures, a larger number of extrusions is required to reach a constant flow rate.

Similar extrusions were made of DMPC solutions at different temperatures and over a range of pressures. Final measurements of $\bar{R}_h$, $\sigma/\bar{\Gamma}$, and the number of extrusions required to reach a constant flow rate are shown in Fig. 3, *a*, *b*, and *c*, respectively, for DMPC extruded at 25°C, 30°C, and 40°C. In general, the size of the vesicles seems to be independent of the temperature of the solution, but decreases significantly as the extrusion pressure increases. It is not possible to extrude significant numbers of DMPC vesicles at or below ~30 psi. At these pressures, some fluid does pass through the polycarbonate filter membranes, but only at an exceedingly low flow rate, and the fluid that is extruded does not contain sufficient vesicles upon which to perform light scattering experiments. Thus there is a minimum pressure P_{min} required to extrude vesicles through narrow pores. The minimum pressure does not vary significantly with temperature. The relative standard deviation as shown in Fig. 3 *b* is independent of both extrusion pressure and temperature. The error bars shown in Fig. 3, *a* and *b*, indicate the standard deviation in values from five measurements. The number of extrusions required to reach a constant flow rate at a given extrusion pressure is shown in Fig. 3 *c*. The number of extrusions required to reach a constant flow rate decreases as the pressure increases, and eventually reaches one extrusion at high pressure at all temperatures. The uncertainties as shown by error bars in the figure are due to uncertainties resulting from flow-rate determination.

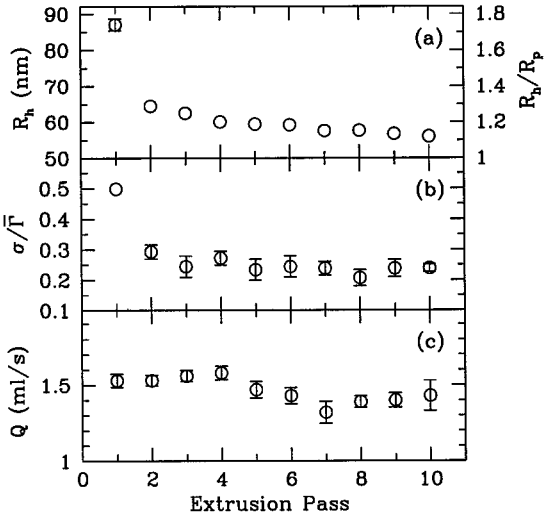

FIGURE 2 Results for (*a*) hydrodynamic radius, (*b*) relative standard deviation, and (*c*) flow rate after each extrusion pass through polycarbonate membranes of nominal radius 50 nm of DMPC in water at a concentration of 1 mg/ml and temperature of 30°C. The applied pressure was 200 psi. The hydrodynamic radius and relative standard deviation equilibrate within about six extrusions. The flow rate is independent of extrusion pass number at this pressure.

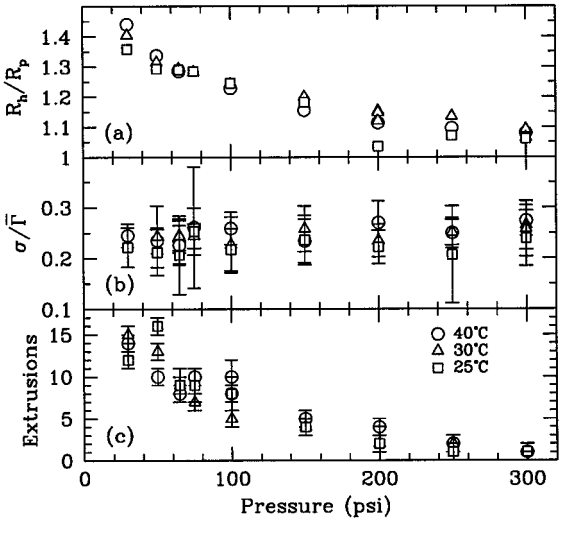

FIGURE 3 Results, for vesicles extruded at different extrusion pressures, of (*a*) hydrodynamic radius, (*b*) relative standard deviation, and (*c*) number of extrusions required to achieve an equilibrium flow rate. DMPC in water at a concentration of 1 mg/ml was extruded through polycarbonate membranes of nominal radius 50 nm at three temperatures: 25°C (□), 30°C (△), and 40°C (○). The hydrodynamic radius and the number of extrusions required to reach an equilibrium flow rate decrease as the applied pressure increases. The relative standard deviation is independent of extrusion pressure.

The DOPC and SOPC solutions behaved in a manner similar to that of the DMPC solution. The results for extrusions carried out at a range of pressures are shown in Fig. 4. At high pressure, the DOPC and SOPC vesicles are slightly larger than the DMPC vesicles extruded at the same pressure, but all samples show a minimum pressure for extrusion and a decrease in radius with extrusion pressure. The minimum pressure required for extrusion varied significantly between lipids. The minimum pressures for which DOPC and SOPC were extruded were ~65 psi and 55 psi, respectively. Fig. 4 *b* shows that there is no change in the relative standard deviation as a function of pressure for any of the phospholipids. The number of extrusions required to reach a constant flow rate was greater for DOPC and SOPC than for DMPC in the intermediate pressure range. At 300 psi, the number of extrusions required to reach constant flow rate was about one for all of the lipids. The number of extrusions required to reach constant flow rate became more disparate near the minimum pressures for extrusion.

The macroscopic bulk flow rate as a function of extrusion pressure is shown for DMPC solutions at various temperatures in Fig. 5 *a* and for different lipids in Fig. 5 *b*. The flow rate of water at 30°C has also been plotted in these figures for the sake of comparison. It is apparent from the figure that the flow rate of the vesicle suspensions is generally smaller than that for water at the same extrusion pressure, and that it depends more strongly on the temperature than on the type of phospholipid.

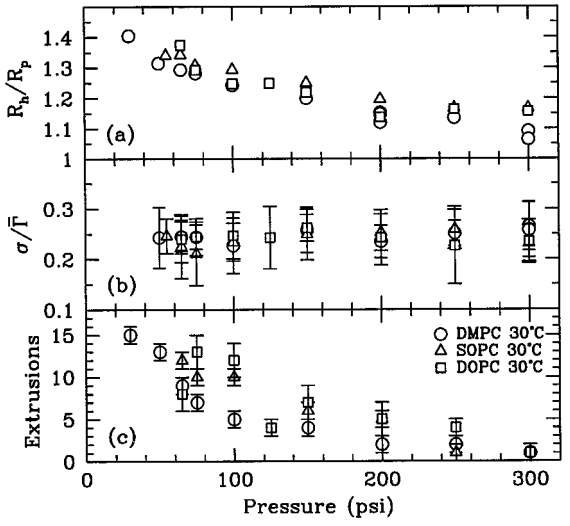

FIGURE 4 Results for vesicles extruded at different extrusion pressures for (*a*) hydrodynamic radius, (*b*) relative standard deviation, and (*c*) number of extrusions required to achieve an equilibrium flow rate. DOPC (□), SOPC (△), and DMPC (○) in water at a concentration of 1 mg/ml were extruded through polycarbonate membranes of nominal radius 50 nm at 30°C. The hydrodynamic radius and the number of extrusions required to reach an equilibrium flow rate decrease as the applied pressure increases. The relative standard deviation is independent of extrusion pressure.

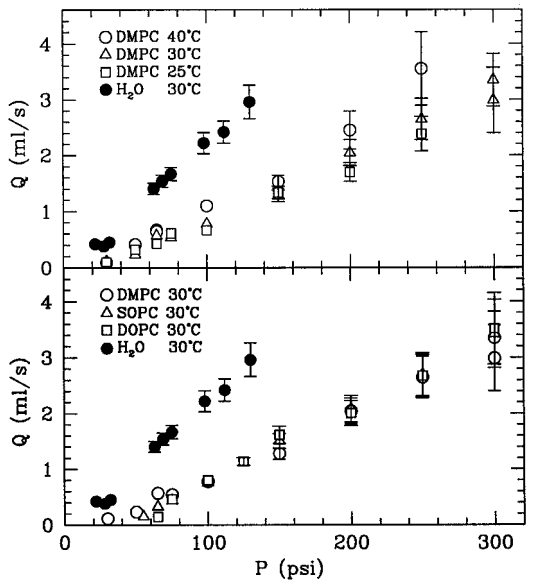

FIGURE 5 Flow rate of vesicle solutions through polycarbonate membranes of nominal radius 50 nm as a function of pressure. (*a*) Comparison of DMPC solutions at different temperatures: 25°C (□), 30°C (△), and 40°C (○). (*b*) Comparison of different lipids: DOPC (□), SOPC (△), and DMPC (○). The flow rate of water is shown as solid circles for comparison. The flow rate of water is typically somewhat higher than that of the vesicle solutions at the same extrusion pressure. The flow rate of water is proportional to the applied pressure over the whole range measured, whereas the flow rate of vesicle solutions is proportional to the applied pressure at pressures above 100 psi.

DISCUSSION

As seen in Fig. 5, the flow rate of water is proportional to the applied pressure over the entire range of applied pressures as predicted by Darcy's law. At high pressures, the flow rates measured for different vesicle solutions are also proportional to the applied pressure. The effective permeability for each sample was calculated from the slope of the high-pressure vesicle solution data (>100 psi), and the permeability for water was calculated from the slope of data taken over the entire pressure range. The results are shown in Table 1. Within experimental errors, values of the effective permeability of the vesicle solutions are consistent with those measured for water. There is no temperature or lipid dependence of the effective permeability of the constant concentration vesicle solutions as predicted by Bruinsma (1996). In fact, the correction factor to the effective perme-

TABLE 1 Effective permeability of polycarbonate membranes to vesicle solutions

Sample	Temperature (°C)	Permeability K (10^{-15} m^4)
Water (Observed)	25	1.53 ± 0.08
DMPC	40	1.11 ± 0.51
DMPC	30	1.37 ± 0.15
DMPC	25	1.47 ± 0.25
SOPC	30	1.57 ± 0.11
DOPC	30	1.52 ± 0.20

ability that is given by the second term in the denominator of Eq. 3 is small at the concentrations used in this study. Using the measured flow rate and assuming that the surface tension is close to the lysis tension, we calculate the correction factor to the effective permeability as given in Eq. 3 to have a magnitude of less than 1%. The temperature dependence of the flow rates measured for different vesicle solutions appears to be due solely to differences in the viscosity of water at different temperatures. This is confirmed in Fig. 6, which shows that the viscosity-corrected flow rates for all vesicle solutions studied are indistinguishable at high pressures. The graph inset shows that variations between samples of different lipids occur at low pressures because of differences in the minimum extrusion pressure. There does not appear to be any significant difference in low pressure data for DMPC samples at various temperatures.

The minimum extrusion pressures P_{min} for the various samples are determined by fitting the viscosity-corrected flow rate ηQ at low pressures (<100 psi) with an empirical function of the form

$$\eta Q = C(P - P_{min})^{\alpha}, \tag{10}$$

where C and α are constants determined by the fitting algorithm. Results for P_{min} are compiled in Table 2. The exponent α is generally around 0.8, but is different for each data set; the data cannot be fit to a single value for α. The results for the minimum pressure for DMPC were obtained by fitting Eq. 10 to the low pressure data for 25°C, 30°C, and 40°C vesicles simultaneously.

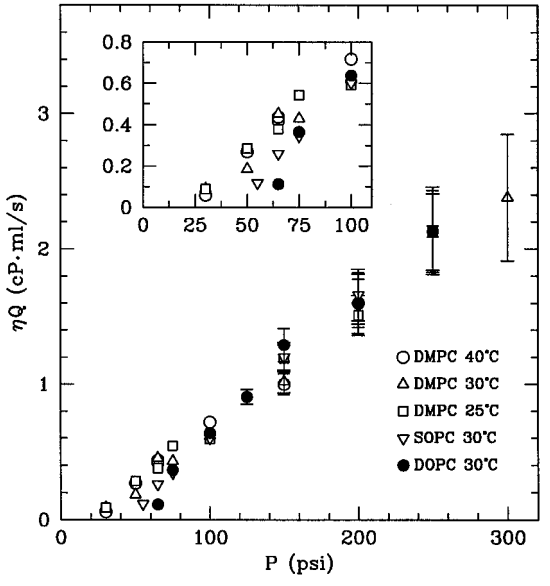

FIGURE 6 Viscosity-corrected flow rate of vesicle solutions through polycarbonate membranes of nominal radius 50 nm as a function of pressure. Comparison of vesicles made from DMPC solutions at different temperatures and from different lipids: 25°C (□), 30°C (△), 40°C (○), DOPC (●), and SOPC (▽). At high pressures, the viscosity-corrected flow rates are indistinguishable. The inset to the graph shows differences in flow rate at low pressure due to different minimum pressures for extrusion.

TABLE 2 Rupture tension of lipid membranes by pipette aspiration and extrusion

Lipid	P_{min} (psi)	Rupture tension (10^{-3} N/m)	
		Pipette aspiration*	Minimum pressure
DMPC	23.1 ± 7.5	2.7 ± 0.8	4.2 ± 1.4
SOPC	49.7 ± 8.6	9.0 ± 1.7	9.0 ± 1.6
DOPC	63.9 ± 1.4	10.2 ± 2.5	11.6 ± 0.25

*Evans and Rawicz (1990).

Intuitively, it is easy to understand why there might be a minimum pressure to extrude vesicles. Fig. 7 shows an idealized depiction of a large vesicle deforming on entering a pore. The multilamellar vesicle that is being extruded is an order of magnitude larger than the size of the pore. This vesicle must be deformed at some energy cost to fit into the smaller pore, and it must undergo a decrease in volume, either by diffusion of water through the membrane or through rupture, to enter the pore. Any of these processes could limit vesicle formation.

The pressure P_b required to bend a vesicle to a given mean radius of curvature R is approximately $P_b \approx \kappa/R^3$, where κ is the elastic bending modulus. The pressure required to deform a large DMPC vesicle with a bending modulus of 1.1×10^{-19} J (Duwe et al., 1990) to fit a pore of radius 50 nm is 0.13 psi. This is two orders of magnitude smaller than any pressure used in the extrusion process, so that it appears that energies associated with bending do not limit this process.

After it is deformed, the volume of the vesicle must decrease before it enters the pore. The volume can decrease because of flow of water through the lipid bilayer or bursting of the bilayer. Flow of water through the bilayer is a slow process, as most of the pressure difference (and subsequent water flow) occurs across the smaller area inside the pore ($2\pi R_p^2$). This leads to a half-life of the volume of the large multilamellar vesicle of ~90 s. This is much slower than any time scale in the extrusion process. On the other

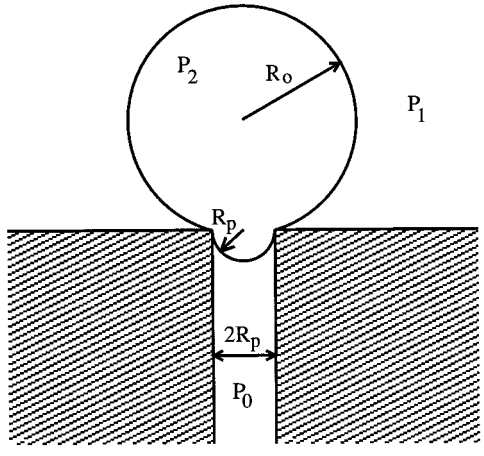

FIGURE 7 Schematic diagram of a vesicle of radius R_o entering a pore of radius R_p. The applied pressure is P_1, the pressure inside the vesicle is P_2, and the pressure in the pore is P_o.

hand, the pressure differences across both the large area outside the pore and the small area inside the pore result in an effective surface tension in the lipid bilayer, as given by the Laplace relation between the pressure difference across a curved interface and the surface tension γ of the interface (Landau and Lifshitz, 1987):

$$\Delta P = 2\gamma H, \tag{11}$$

where H is the mean curvature of the interface. Consideration of the differences in pressures $P_2 - P_1$ and $P_2 - P_0$, where P_1 is the applied pressure, P_2 is the pressure inside the vesicle, and P_0 is atmospheric pressure, and the assumption that the surface tension is constant throughout the bilayer yields an expression for the applied pressure difference $P_1 - P_0$ in terms of the pore radius R_p and the radius of the outer portion of the vesicle R_o,

$$P_1 - P_0 = 2\gamma\left[\frac{1}{R_p} - \frac{1}{R_o}\right] \approx 2\gamma\frac{1}{R_p}. \tag{12}$$

If the tension grows larger than the lysis tension of the bilayer, the bilayer will rupture and the vesicle will be able to proceed through the pore. Lysis tensions calculated from Eq. 12 using values of P_{min} from Table 2 are also shown in Table 2. Comparison with values for lysis tensions obtained from pipette aspiration experiments of single, large ($\sim$10 μm) vesicles (Evans and Rawicz, 1990) show that the results agree within experimental uncertainties. It appears that the minimum extrusion pressure corresponds to the pressure, which results in a surface tension sufficient to cause vesicle rupture.

The observation that vesicle size decreases with flow rate is consistent with observations made in other studies of lamellar phases (Diat et al., 1993) and emulsions (Mason and Bibette, 1996) under shear, although the physical mechanism responsible for this behavior may be different in this case. Certainly as the flow rate increases, Eq. 4 predicts that the lubrication layer should increase in thickness, so that the vesicle tube decreases in radius. We believe that this tube will break into smaller tubes or plugs as the induced surface tension becomes larger than the lysis tension of the lipid bilayers, and that the size of this tube should determine the radius of the final vesicles.

CONCLUSIONS

We have made measurements of the size and polydispersity of extruded vesicles as a function of extrusion pressure, lipid composition, and temperature. We find that it is not possible to extrude vesicles below a lipid-dependent minimum pressure that corresponds to the lysis tension required to rupture the bilayer membrane. This provides a convenient way to measure lysis tensions. As the extrusion pressure is increased, the flow rate of vesicles through the pores increases and the size of the extruded vesicles decreases. At high pressures, the pressure dependence of the viscosity-corrected flow rate of all equal-concentration lipid mixtures is indistinguishable. The decrease in vesicle size with extrusion pressure is consistent with other studies of complex fluids under shear (Diat et al., 1993; Mason and Bibette, 1996). There does not seem to be a significant difference in vesicle size for vesicles made of the different lipids tested here when they are extruded at the same concentration and extrusion pressure. Previous observations of variations in vesicle size may have been due to different extrusion pressures or concentrations. Finally, the polydispersity of the vesicle size distribution is independent of extrusion pressure and lipid properties, and is most likely intrinsic to the filter membranes.

The authors gratefully acknowledge helpful conversations with Art Bailey, Robijn Bruinsma, and Michael Wortis, and the assistance of Ana Siu with some of the measurements.

This research was supported by Natural Sciences and Engineering Research Council of Canada.

REFERENCES

Berne, B. J., and R. Pecora. 1976. Dynamic Light Scattering. John Wiley and Sons, New York.

Bruinsma, R. 1996. Rheology and shape transitions of vesicles under capillary flow. *Physica A.* 234:249–270.

Clerc, S. G., and T. E. Thompson. 1994. A possible mechanism for vesicle formation by extrusion. *Biophys. J.* 67:475–477.

Diat, O., D. Roux, and F. Nallet. 1993. Effect of shear on a lyotryopic lamellar phase. *J. Phys. II.* 3:1427–1452.

Duwe, H. P., J. Kaes, and E. Sackmann. 1990. Bending elastic moduli of lipid bilayers: modulation by solutes. *J. Phys.* 51:945–962.

Evans, E., and W. Rawicz. 1990. Entropy-driven tension and bending elasticity in condensed-fluid membranes. *Phys. Rev. Lett.* 64:2094–2097.

Gompper, G., and D. M. Kroll. 1995. Driven transport of fluid vesicles through narrow pores. *Phys. Rev. E.* 52:4198–4208.

Hope, M. J., M. B. Bally, G. Webb, and P. R. Cullis. 1985. Production of large unilamellar vesicles by a rapid extrusion procedure: characterization of size, trapped volume and ability to maintain a membrane potential. *Biochim. Biophys. Acta.* 812:55–65.

Koppel, D. E. 1972. Analysis of macromolecular polydispersity in intensity correlation spectroscopy: the method of cumulants. *J. Chem. Phys.* 57:4814–4820.

Küolchens, S., V. Ramaswami, J. Birgenheier, L. Nett, and D. F. O'Brien. 1993. Quasi-elastic light scattering determination of the size distribution of extruded vesicles. *Chem. Phys. Lipids.* 65:1–10.

Landau, L., and E. Lifshitz. 1987. Fluid Mechanics, 2nd Ed. Pergamon Press, Oxford.

MacDonald, R. C., R. I. MacDonald, B. Ph. M. Menco, K. Takeshita, N. K. Subbarao, and L. Hu. 1993. Small-volume extrusion apparatus for preparation of large, unilamellar vesicles. *Biochim. Biophys. Acta.* 1061:297–303.

Mason, T. G., and J. Bibette. 1996. Emulsification of viscoelastic media. *Phys. Rev. Lett.* 77:3481–3484.

Mayer, L. D., M. J. Hope, and P. R. Cullis. 1986. Vesicles of variable sizes produced by a rapid extrusion procedure. *Biochim. Biophys. Acta.* 858: 161–168.

Mui, B., P. R. Cullis, E. A. Evans, and T. D. Madden. 1993. Osmotic properties of large unilamellar vesicles prepared by extrusion. *Biophys. J.* 64:443–453.

Nayer, R., M. J. Hope, and P. R. Cullis. 1989. Generation of large unilamellar vesicles from long-chain saturated phosphatidylcholines by extrusion techniques. *Biochim. Biophys. Acta.* 986:200–206.

New, R. R. C. 1995. Influence on liposome characteristics on their properties and fate. *In* Liposomes as Tools in Basic Research and Industry. J. R. Philippot and F. Schuber, editors. CRC Press, Boca Raton, FL. 19.

Woodle, M. C., M. S. Newman, and P. K. Working. 1995. Biological properties of sterically stabilized liposomes. *In* Stealth Liposomes. D. Lasic and F. Martin, editors. CRC Press, Boca Raton, FL. 106.